

H₂ blister formation on metallic surfaces – a candidate for degradation processes in space

Maciej Sznajder¹ and Ulrich Geppert.²

DLR Institute for Space Systems, System Conditioning, Robert-Hooke-Str. 7, 28359 Bremen, Germany

University of Zielona Góra, Kepler Institute of Astronomy, Lubuska 2, 65-265, Zielona Góra, Poland

H₂-blisters are metal bubbles filled with hydrogen molecular gas resulting from recombination processes of protons in metal lattice. Bubble formation depends on many physical parameters, for instance: proton energy, proton flux, or the temperature of an exposed sample. Up to now no metallic sample that has been exposed to conditions prevalent in the interplanetary medium has been returned to Earth. Therefore, a direct evidence that blistering appears in space is missing. However, blistering is certainly a candidate of degradation processes which may occur in space. It could play an important role in the solar sail technology, where the performance of the sail is significantly affected by both the sail geometry but especially by optical properties of sail materials. Thus, both theoretical and laboratory studies of the blistering process have to be performed.

The here presented model simulates the growth of molecular hydrogen bubbles on metallic surfaces. Additionally, it calculates the decrease of reflectivity of the by blistering degraded foils. First theoretical results show that the reflectivity of an Aluminum foil decreases by about 27% for a bubble surface density of 1500 cm⁻² and an average bubble radius of 100 μm. Therefore, if blistering occurs, the propulsion performance of any sail-craft will be decreased by a significant factor.

Nomenclature

A	=	area of the sample
BS	=	backscatter coefficient
d_{csda}	=	Continuous Slowing Down Approximation (CSDA-range)
η	=	relation between the number of H ₂ molecules and the H atoms in the metal lattice

¹ Scientist Maciej.Sznajder@dlr.de, tel.: +49 421 24420-1623

² Professor Ulrich.Geppert@dlr.de, tel.: +49 421 24420-1604

ϵ	=	binding energy of the H ₂ molecule to a vacancy
ϵ'	=	migration energy of the H atom in the metal lattice
ϵ_{cell}	=	size of a grid cell that covers the irradiated sample
E	=	Young module
E_{int}	=	Internal energy of molecules/atoms located at certain positions in the metal lattice
$F_{\text{gas},i}$	=	free energy of gas inside the i th bubble
F_{H}	=	free energy of H atoms located outside bubbles in the metal lattice
F_{H_2}	=	free energy of H ₂ molecules located outside bubbles in the metal lattice
$F_{\text{md},i}$	=	free energy of metal deformation caused by expanding i th bubble
$F_{\text{surf},i}$	=	surface free energy of the i th bubble cap
γ	=	Poisson coefficient
H_i	=	sum of partial derivatives
I	=	proton flux
k_{B}	=	Boltzmann constant
M_{u}	=	molar mass of the sample's material
N	=	number of iterations
N_0	=	number of lattice sites
N_{B}	=	number of bubbles per unit area
N_{B}^{T}	=	total number of bubbles at the irradiated sample
N_{cell}	=	number of cells
N_{H}^{T}	=	total number of H atoms in the sample
$N_{\text{H}_2}^{\text{T}}$	=	total number of H ₂ molecules in the sample
$\Delta N_{\text{p}^+,j}$	=	number of protons sent to the sample in a unit time period
p_i	=	pressure of the gas inside the i th bubble
q	=	momentum
Δq_i	=	momentum transfer of a photon to the i th cell of the degraded foil
$\Delta q_{\text{max},i}$	=	momentum transfer of a photon to the i th cell of a perfect mirror
\bar{r}	=	average bubble radius
$r_{i,0}$	=	initial radius of the bubble

R	=	reflectivity
S	=	entropy
σ	=	metal strain
θ	=	angle between the surface normal and the path of a light ray
Δt_j	=	time step
T	=	temperature of the sample
V_i	=	volume of the i^{th} bubble
$V_{\text{max},i}$	=	maximum volume of the i^{th} bubble
V_{min}	=	minimum volume of a bubble
ξ	=	relation between the number of H_2 molecules inside and outside the bubbles
$\Xi_{i,j}$	=	increment of increase of the i^{th} bubble radius during the j^{th} period of time

I. Introduction

Materials covered with metallic surfaces are often used in space technology. For instance, thin Polyimide foils like Kapton, covered on both sides with a thin Aluminum layer, are manufactured for solar sails. The performance of the sails is significantly affected by both the sail geometry and the optical properties of its surface materials [4]. Degradation processes will change the physical properties of these materials. Studies, both theoretical and experimental, allow to choose the best material for a given sail mission.

Degradation of structural properties of solids caused by hydrogen, (referred to as embrittlement) plays a fundamental role in materials physics [12]. Materials used in space technology are exposed to hazard and aggressive conditions like high-energetic radiation or rapid temperature changes. Bubble formation is one of four general processes of embrittlement [12]. When H_2 -bubbles are formed on the surface of an irradiated solar sail, its reflectivity decreases with increasing surface density of molecular hydrogen bubbles. Since the reflectivity is directly proportional to the momentum transfer from solar photons to the sail, its decrease will reduce the propulsion performance of a sail-craft just linearly proportional to the reduction of the reflectivity.

For the bubble formation certain conditions with respect to sail temperature and dose of sail penetrating protons have to be fulfilled. It turns out, that bubble formation is very likely at least at distances from the Sun smaller than 1.5 AU, perhaps even for somewhat larger distances.

The here presented thermodynamic model describes the growth of H_2 -bubbles. The model input parameters are the energy and flux of solar protons, properties of the irradiated metal, the dose of protons penetrated into the

metal, and its temperature. Another input parameter is the number of vacancies in the subsurface layers of the metal. Only at vacancy sites bubbles can be formed, i.e. their surface density is determined by the vacancy density which, in turn, is determined by the quality of the metal production process.

The model output is the velocity of bubble radius growth, the maximum possible bubble radius, and, for a given bubble density and average bubble radius, the reduction factor of the reflectivity with respect to its ideal value.

II. Temporal evolution of bubble formation

Incident protons, while penetrating the metallic target, recombine with its free electrons to neutral hydrogen atoms. There are four recombination processes of ions to neutral atoms: Auger- [6, 7, 8, 16, 17, 22], resonant- [6, 23], Oppenheimer-Brinkman-Kramers (OBK) - [1, 9], and Radiative Electron Capture (REC) [9] – recombination. Each one has its own probability of occurrence. It depends crucially on the energy of the incident ion. According to cross sections studies, the first two processes dominate the recombination of solar protons with energies lower than 100 keV. Above 100 keV the OBK process together with REC process (this even only above a few MeV) dominates recombination. The solar proton flux has its maximum at about 1 keV (see Fig. 1). At 100 keV it is already two orders of magnitude lower. Therefore, recombination studies of solar protons should be focused on Auger- and resonant – recombination processes.

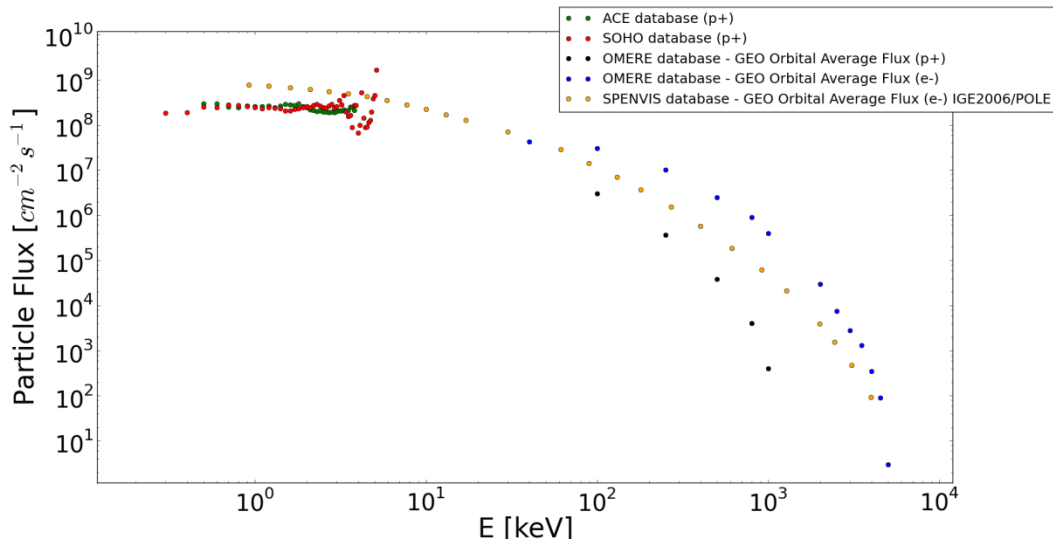


Fig. 1 Flux of solar protons and electrons as a function of energy. Data are taken from the databases of SOHO, ACE, OMERE, and SPENVIS.

Blistering occurs as irradiation damage. It changes the physical properties of the irradiated surface and increases the erosion rate [2]. Blistering is caused by formation of pockets of hydrogen molecular gas just below

the metal surface. There have been made many terrestrial irradiation experiments by use of Hydrogen ions as incident particles. Many types of target metallic materials have been investigated. An example of a population of bubbles is shown in the Fig. 2 [15]. Bubbles were formed on the 2 μm thick Aluminum sample after the critical dose of incident Hydrogen ions was reached. The Hydrogen ions energy was set to 1 keV; the sample was hold at a temperature of 300 K.

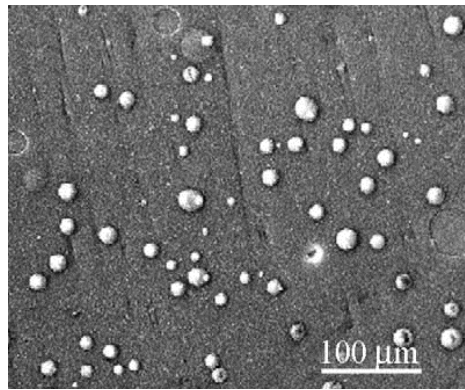


Fig. 2 Typical population of molecular hydrogen bubbles on an Aluminum sample. The diameter of the bubbles is in the range of a few μm [15].

The tendency to form bubbles depends on the proton energy, integrated proton flux (dose), temperature of the target, crystallographic orientation of the irradiated surface as well as on impurities and defects in the sample [5]. It is known from laboratory experiments that the minimum dose of protons above which the process occurs is $\sim 10^{16} \text{ H}^+ \text{ cm}^{-2}$ e.g. [14]. The temperature range in which bubbles were observed is between 288 and 573 K [5, 14].

Hydrogen atoms are much smaller than metal atoms, but they can introduce strain in metal lattices when being absorbed as interstitial atoms [21, 25]. They can also change the electronic structure of near neighbor metal atoms [21]. That causes an increase of the lattice energy. It may be decreased by the aggregation of the interstitial hydrogen atoms into hydrogen atom clusters, and then into molecular hydrogen bubbles [21]. Hydrogen could not agglomerate into H_2 -clusters without the presence of vacancies. For instance a single vacancy in Aluminum can trap up to twelve H atoms. For comparison, a vacancy in Iron can trap only up to six H atoms [12].

Here, a thermodynamic model of bubble growth is proposed. The model is based on the assumption that the growth proceeds quasi-static i.e. during a j^{th} period of time Δt_j a small portion of H_2 -molecules, $N_{\text{H}_2,i,j}$, is added to the i^{th} bubble. The thermodynamic equilibrium, however, is re-established very fast after each addition. For

simplicity it is assumed that a single bubble is a half of the sphere with a radius of r_i . The gas within a bubble behaves to a good approximation like an ideal gas:

$$p_i V_i = \sum_j^N N_{H_2,i,j} k_B T, \quad (1)$$

The total irradiation time of the sample, during which the bubble growth appears, is $N \times \Delta t_j$. The number $N_{H_2,i,j}$ is given by:

$$N_{H_2,i,j} = 0.5(N_B^T)^{-1} \Delta N_{p^+,j} \eta \xi (1 - BS), \quad N_B^T = N_B A, \quad \Delta N_{p^+,j} = I \Delta t_j A. \quad (2)$$

Here 0.5 reflects that a single H_2 -molecule consists of two H atoms. While 100% of protons recombine into H atoms in the metal lattice, only a few percent of them recombine to H_2 -molecules [3]. Hence, the coefficient η is the ratio between the number of H_2 -molecules and the H-atoms in the lattice. Not all of the H_2 -molecules will merge into H_2 -clusters and finally form H_2 -bubbles. Thus, the coefficient ξ denotes the ratio of the number of H_2 -molecules inside and outside the bubbles.

The first step to estimate the radius growth of the i^{th} bubble is to calculate the Helmholtz free energy of the whole configuration F_{config} . Since the free energy is an additive quantity, the total free energy of bubble formation is a sum of following quantities: free energy of H_2 gas inside the i^{th} bubble ($F_{\text{gas},i}$), of the metal surface deformation ($F_{\text{md},i}$) caused by the bubble growth itself, of the surface free energy ($F_{\text{surf},i}$) of the bubble cap, of the free energy of H_2 -molecules (F_{H_2}), and of H-atoms (F_H) placed outside the bubbles but within the metal lattice. The Helmholtz free energy of the whole configuration described above is then:

$$F_{\text{config}} = F_{\text{gas},i} + F_{\text{md},i} + F_{\text{surf},i} + F_{H_2} + F_H. \quad (3)$$

The next step is to estimate the free energy of the i^{th} bubble growth. It consists of the free energy of a gas filled in the bubble, the free energy of metal deformation, and of the bubble cap surface free energy. Using the thermodynamic relation between pressure of a gas and its Helmholtz free energy $p = \left(\frac{\partial F}{\partial V}\right)_T$ together with the ideal gas equation of state (Eq. (1)), the free energy of a gas within the i^{th} bubble is

$$F_{\text{gas},i} = - \sum_j^N N_{H_2,i,j} k_B T \ln \left(\frac{V_{\text{max},i}}{V_{\text{min}}} \right), \quad (4)$$

The model assumes that two H_2 molecules form the smallest (“initial”) possible bubble. The radius of such a bubble is approximately 3.2 Bohr radii [20]. Every bubble will crack if the pressure of the gas inside is higher than the pressure exerted by the metal deformation of the cap. The relation between the pressure of the gas, the strain σ of the metal, and the bubble radius corresponding to $V_{\text{max},i}$ is [11]:

$$p_{\text{gas, inside bubble}} - p_{\text{outside bubble}} = \frac{2\sigma}{r_{\text{max},i}}. \quad (5)$$

Since the sample is placed in the vacuum, the pressure outside the bubble is set to zero.

The free energy of metal deformation caused by the gas pressure inside the bubble with radius r_i can be found in [10], and is given by the following relation:

$$F_{\text{md},i} = \frac{4\pi r_i^3 (1+\gamma)}{3E} p_i^2. \quad (6)$$

The free energy of a surface of a cap of the i^{th} bubble is given by [13]:

$$F_{\text{surf},i} = 4\pi r_i^2 \sigma(T). \quad (7)$$

The Helmholtz free energy of the H_2 -molecules located at certain positions in the metal lattice but outside the bubbles is calculated in the form $F = E_{\text{int}} - TS$. Applying the statistical definition of the entropy, this free energy is (for a detailed derivation see M. Sznajder, thesis 2013 [24]):

$$F_{\text{H}_2} = \left(N_{\text{H}_2}^{\text{T}} - \sum_i N_{\text{B}}^{\text{T}} \sum_j N_{\text{H}_2,i,j}^{\text{N}} \right) \left[\varepsilon + k_{\text{B}} T \ln \left(\frac{N_{\text{H}_2}^{\text{T}} - \sum_i N_{\text{B}}^{\text{T}} \sum_j N_{\text{H}_2,i,j}^{\text{N}}}{N_0} \right) \right]. \quad (8)$$

The number of lattice sites N_0 can be expressed by:

$$N_0 = N_{\text{A}} d_{\text{csda}} \frac{A^2}{M_{\text{u}}}. \quad (9)$$

The Helmholtz free energy of H atoms located at certain positions within the metal lattice is calculated in the same way as for Eq. (8):

$$F_{\text{H}} = \left(N_{\text{H}}^{\text{T}} - 2N_{\text{H}_2}^{\text{T}} \right) \left[\varepsilon' + k_{\text{B}} T \ln \left(\frac{N_{\text{H}}^{\text{T}} - 2N_{\text{H}_2}^{\text{T}}}{N_0} \right) \right]. \quad (10)$$

Since now each term of Eq. (3) is determined, the next step is to calculate the radius r_i of the i^{th} bubble at a given time t . This will be achieved by assuming that the process of bubble growth is quasi-static one, i.e. during each j^{th} time step Δt_j a small portion of H_2 molecules is merged to the i^{th} bubble and the thermodynamic equilibrium is rapidly re-established; the corresponding equilibrium condition is $\frac{\partial F_{\text{config}}}{\partial N_{\text{H}_2,i,j}} = 0$. This leads to the

following fifth order equation for r_i :

$$8\pi \Xi_{i,j} \sigma(T) r_i^5 - H_i r_i^4 + \frac{3}{\pi} \frac{1+\gamma}{E} \left(\sum_j N_{\text{H}_2,i,j}^{\text{N}} \right) k_{\text{B}}^2 T^2 [2N r_i - 3\Xi_{i,j} \sum_j N_{\text{H}_2,i,j}^{\text{N}}] = 0. \quad (11)$$

$\Xi_{i,j}$ is defined below in Eq. (13). H_i denotes the abbreviation:

$$H_i = - \frac{\partial F_{\text{gas},i}}{\partial N_{\text{H}_2,i,j}} - \frac{\partial F_{\text{H}}}{\partial N_{\text{H}_2,i,j}} - \frac{\partial F_{\text{H}_2}}{\partial N_{\text{H}_2,i,j}}. \quad (12)$$

III. Formation possibility of H₂ bubbles in the interplanetary medium, numerical analysis of bubble growth.

Growth of molecular hydrogen bubbles will be possible in the interplanetary space if the criterion of the minimum dose of protons is fulfilled. The temperature of the sample has to be high enough to start the bubble formation, but not too high to lose Hydrogen much too rapidly due to the high diffusivity of Hydrogen in metals.

To estimate, whether the conditions for bubble formation are fulfilled a thin 1m × 1m non-rotating Aluminum foil (10 μm thick) is assumed to be located at 1 AU distance from the Sun. The foil surface normal is directed toward the Sun. The foil temperature will reach rapidly an equilibrium value of 520 K. Thus, the temperature criterion is fulfilled. Solar proton flux data, collected by the SOHO and ACE mission, return a typical flux at 5 keV of about 10⁹ H⁺ cm⁻² s⁻¹ (see Fig. 1). Under the simplifying assumption that the Sun generates only mono-energetic 5 keV protons, the criterion of minimum proton dose will be fulfilled after 116 days. In reality this happens even earlier (for a detailed analysis see M. Sznajder, thesis 2013 [24]). Therefore, both the temperature and the dose criterion for bubble formation are fulfilled if metallic surfaces are exposed to the solar wind in typical Earth distances from the Sun.

For the modeling of bubble growth, the *i*th bubble located on the Aluminum surface (area 1cm²) consists at time t=0 only of two H₂-molecules, in accordance with an assumption about *V*_{min}. At each time step Δ*t*_{*j*} a small number of H₂ molecules are merged to the bubble. Therefore, Eq. (11) has to be solved at each time step. A realistic assumption of bubble growth dynamics is:

$$\Xi_{i,j} = \frac{\Delta r_i}{\Delta N_{H_2,i,j}} = j^{\frac{1}{3}} r_{i,0}. \quad (13)$$

The exponent $\frac{1}{3}$ is a model parameter of bubble growth; it is a good guess according to the experimentally found gas pressures inside the bubbles [18]. An increase of that exponent leads to a reduction of the pressure of the gas in the bubble. Six models are presented here. For each model it is assumed that the sample has been irradiated by a proton flux of 6.24×10^{12} H⁺ cm⁻² s⁻¹ during more than 10⁴ seconds. Hence the criterion of critical dose of protons above which the bubble formation can proceed is fulfilled. Two different temperatures of the sample are considered: 300, and 550 K. The *BS* coefficient is set to 10⁻². This value has been estimated by use of the SRIM software [26]. The coefficient η which determines the ratio of H₂-molecules to H-atoms is set to 10⁻², a value which is taken from the work of Canham et al. [3]. In order to study a wide range of the availability of vacancies within the lattice, the free parameter ξ, which prescribes the ratio of H₂-molecules inside and outside the bubbles, is set to: 10⁻⁶, 10⁻⁴, and 10⁻².

The results are presented in Fig. 3. While the left plot shows the temporal evolution of bubble growth at 300 K, the right plot presents it at 550 K. Blue-, green-, and red- lines denote models with ξ -factor of: 10^{-6} , 10^{-4} , and 10^{-2} , respectively. A significant influence on to the bubble growth has the ξ - factor. To illustrate this compare for a temperature of 300K the radii after an irradiation period of 10^4 s. For $\xi = 10^{-4}$ the bubble radius is by a factor of about 5 larger than for $\xi = 10^{-6}$. In case of $\xi = 10^{-2}$ this factor increases to 30. Clearly, the larger the fraction of H_2 -molecules that find their way into a bubble, the faster it grows. An increase in temperature has an effect in the like direction. After the same irradiation period and for $\xi = 10^{-2}$ is the radius at 550K about 33% larger than at 300K. Obviously, as long as the upper threshold is not exceeded, the bubble formation benefits from a higher temperature of the metal.

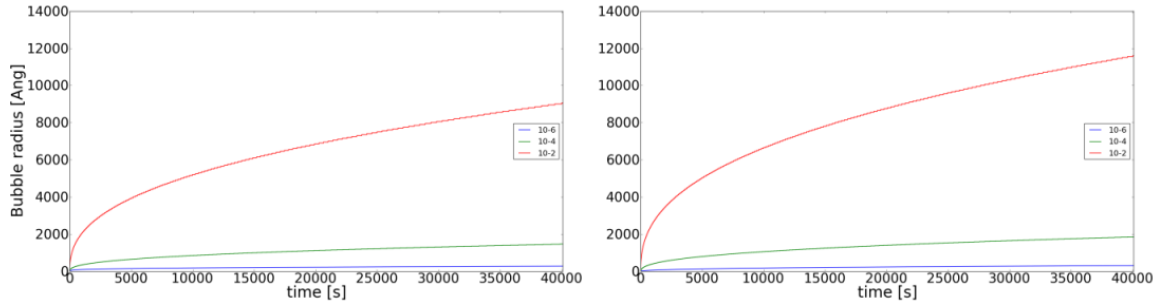


Fig. 3 Bubble radius as function of time. Left panel: T=300K, right panel: T=550K. The blue, green and red curves correspond to ξ -parameters of 10^{-6} , 10^{-4} , and 10^{-2} , respectively.

IV. The effect of bubble formation on to the reflectivity

The momentum transfer of a photon to an ideal reflecting surface is given by $\Delta q = 2q \cos \theta$, where the factor 2 is just in accordance with specular reflectivity. Certainly, the surface quality will suffer during the irradiation with protons from progressing bubble formation. At time $t = 0$ the foil has not been exposed to the electromagnetic radiation and/or charged particles, and is considered to be a perfect mirror with reflectivity $R = 1$. That means that all of the incident light rays are reflected perfectly, no light ray is absorbed or diffusively reflected by the target. Later, when the foil has been irradiated by a flux of protons and molecular hydrogen bubbles have been formed on its surface, the reflectivity of the degraded foil will be reduced. This deterioration is calculated in the following way: the foil is covered by a grid with a fixed single cell size of $\varepsilon_{\text{cell}} \times \varepsilon_{\text{cell}}$ (see Fig 4).

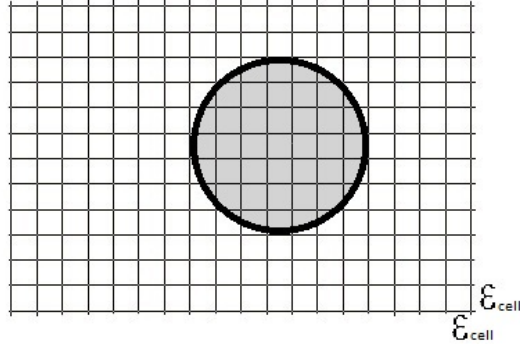


Fig. 4 Grid covered fraction of the foil with one spherical bubble. The cell area is $\epsilon_{\text{cell}} \times \epsilon_{\text{cell}}$.

The reflectivity of a single cell is by definition $\frac{\Delta q}{\Delta q_{\text{max}}}$. Hence, taking into account all cells, one has:

$$R_{\text{foil}} = \frac{\sum_i^{N_{\text{cell}}} \Delta q_i}{\sum_i^{N_{\text{cell}}} \Delta q_{\text{max},i}} \quad (14)$$

The path of photons is directed parallel to the foil surface normal. Therefore, at time $t = 0$ the foil was a perfect mirror without surface imperfections and $\theta_i = 0$. Later, when the surface is populated with bubbles, θ_i will vary between 0 and 90° . Thus, Eq. (14) reduces to:

$$R_{\text{foil}} = \frac{\sum_i^{N_{\text{cell}}} 2q \cos \theta_i}{N_{\text{cell}} \times 2q} = \frac{\sum_i^{N_{\text{cell}}} \cos \theta_i}{N_{\text{cell}}} \quad (15)$$

The reduction of reflectivity is here demonstrated for three different bubble number densities N_B : 500 cm^{-2} , 1000 cm^{-2} , and 1500 cm^{-2} . The ratio of the average radius of the bubble \bar{r} to the size of the cell ϵ_{cell} is fixed and set to 100. Results are presented in Fig. 5. It turns out that the reflectivity is quite sensitive to the average radius and surface density of bubbles that cover the irradiated foil. For a small average radius of bubbles the change in the reflectivity is negligibly small. However, for bubbles with an average radius of $100 \mu\text{m}$ the change in the reflectivity with respect to the initial state of the foil is significant: 7%, 17%, and 27% for $N_B = 500 \text{ cm}^{-2}$, 1000 cm^{-2} , and 1500 cm^{-2} , respectively.

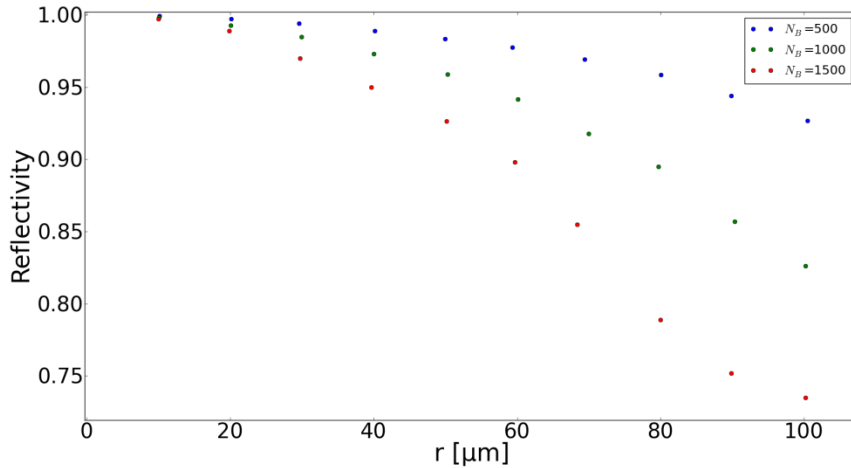


Fig. 5 Reflectivity of a metallic foil covered with hydrogen molecular bubbles as function of the average bubble radius for three bubbles surface densities N_B : 500 cm^{-2} , 1000 cm^{-2} , and 1500 cm^{-2} .

V. Conclusion

The main conclusion is that the bubble growth phenomenon and its consequence, the blistering, may have a serious influence on the propulsion efficiency of any sail-craft. The here presented model calculations have shown that blistering may appear on metallic surfaces exposed to the solar wind in the close vicinity of the Sun (detail calculations presented in Maciej Sznajder's thesis [24] has shown that the blistering process may occur in orbits between 0.5 AU and 1.5 AU). Under conditions that prevail there, high bubble surface densities with average bubble radius in the μm range can be expected. The corresponding reduction of the sail reflectivity must be considered in the planning of solar sail missions.

Acknowledgments

Maciej Sznajder is a scholar within Sub-measure 8.2.2 Regional Innovation Strategies, Measure 8.2 Transfer of knowledge, Priority VIII Regional human resources for the economy Human Capital Operational Programme co-financed by European Social Fund and state budget.

We are grateful to Martin Siemer for modeling the thermal behavior of a sail at 1 AU.

References

- [1] Alston S., "Theory of Electron Capture from a Hydrogenlike Ion by a Bare Ion: Intermediate-State Contributions to the Amplitude", *Physical Review A*, Vol. 27, No. 5, 1983, pp. 2342-2357, doi: 10.1103/PhysRevA.27.2342,
- [2] Astrelin V. T. et al., „Blistering of the selected materials irradiated by intense 200 keV proton beam“, *Journal of Nuclear Material*, Vol. 396, No. 1, 2010, pp. 43-48, doi: 10.1016/j.jnucmat.2009.10.051

- [3] Canham L. T., Dyball M. R., Leong W. Y., Houlton M. R., Cullis A. G., Smith P. W., "Radiative Recombination Channels due to Hydrogen in Crystalline Silicon", Vol. 4, No. 1-4, 1989, pp. 41-45, doi: 10.1016/0921-5107(89)90213-4
- [4] Dachwald B., Macdonald M., McInnes C. R., Mendali G., Quarta A. A., „Impact of Optical Degradation on Solar Sail Mission Performance“, *Journal of Spacecraft and Rockets*, Vol. 44, No. 4, 2007, pp. 740-749, doi: 10.2514/1.21432
- [5] Daniels R. D., "Correlation of Hydrogen Evolution with Surface Blistering in Proton-Irradiated Aluminium", *Journal of Applied Physics*, Vol. 42, No. 1, 1971, pp. 417-419, doi: 10.1063/1.1659613
- [6] Echenique P. M., Flores F., "Inelastic Proton-Solid Collisions", *Physical Review B*, Vol. 35, No. 15, 1987, pp. 8249-8251, doi: 10.1103/PhysRevB.35.8249
- [7] Guinea F., Flores F., Echenique P. M., "Charge States for H and He Moving in an Electron Gas", *Physical Review B*, Vol. 25, No. 10, 1982, pp. 6109-6125, doi: 10.1103/PhysRevB.25.6109
- [8] Hagstrum D. "Theory of Auger Ejection of Electrons from Metals by Ions", Vol. 96, No. 2, 1954, pp. 336-365, doi: 10.1103/PhysRev.96.336
- [9] Kuang Y. R., "Model-Potential Oppenheimer-Brikman-Kramers Approximation for K-shell Electron Capture in Asymmetric Collisions", *Physical Review A*, Vol. 44, No. 3, 1991, pp. 1613-1619, doi: 10.1103/PhysRevA.44.1613
- [10] Landau L. D., Lifschitz M. J., *Theory of Elasticity*, 2nd ed., Pergamon Press, Oxford, 1970
- [11] Lautrup B., *Physics of Continuous Matter*, 2nd ed., Taylor & Francis Group, Boca Raton, Florida, USA, 2011
- [12] Lu G., Kaxiras E., "Hydrogen Embrittlement of Aluminium: The Crucial Role of Vacancies", *Physical Review Letters*, Vol. 94, No. 15, 2005, pp. 155501-155504, doi: 10.1103/PhysRevLett.94.155501
- [13] Martynenko Yu. V., "The Theory of Blister Formation", *Radiation Effects*, Vol. 45, 1979, pp. 93-102, doi: 10.1080/00337577908208414
- [14] Milacek L. H., Daniels R. D., Cooley J. A., "Proton-Radiation-Induced Blistering of Aluminum", *Journal of Applied Physics*, Vol. 39, No. 6, 1967, pp. 2803-2816, doi: 10.1063/1.1656677
- [15] Milcius D., Pranevicius L. L., Templier C., "Hydrogen storage in the bubbles formed by high-flux ion implantation in thin Al films", *Journal of Alloys and Compounds*, Vol. 398, No. 1, 2005, pp. 203-207, doi: 10.1016/j.jallcom.2005.02.003
- [16] Pauly N., Dubus A., Rösler M., „Electron Capture and Loss Processes for Protons in Aluminium: Comparison Between Conduction Band Electron-Hole Assisted and Plasmon Assisted Auger Processes“, *Nuclear Instruments and Methods in Physics Research Section B: Beam Interactions with Materials and Atoms*, Vol. 193, No. 1-4, 2002, pp. 414-418, doi: 10.1016/S0168-583X(02)00814-5
- [17] Penalba M., Anrau A., Echenique P. M., "Target Dependence of Electron-Capture and -Loss Cross Sections of Protons in Solids", *Nuclear Instruments and Methods in Physics Research Section B: Beam Interactions with Materials and Atoms*, Vol. 48, No. 1-4, 1990, pp. 138-141, doi: 10.1016/0168-583X(90)90091-8

- [18] Primak W., "Facies of Ion Bombarded Bombarded Surfaces of Brittle Materials", *Solid State Science Division*, 1975, Argonne National Laboratory, Argonne, Illinois 60439, USA
- [19] Raisbeck G., Yiou F., "Electron Capture by 40-, 155-, and 600-MeV Protons in Thin Foils of Mylar, Al, Ni, and Ta", *Physical Review A*, Vol. 4, No. 5, 1971, pp. 1858-1868, doi: 10.1103/PhysRevA.4.1858
- [20] Ree F. H., Bender C. F., "Repulsive intermolecular potential between two H₂ molecules", *Journal of Chemical Physics*, Vol. 71, No. 12, 1979, pp. 5362-5376, doi: 10.1063/1.438349
- [21] Ren X., Chu W., Li J., Su Y., Qiao L., „The Effects of Inclusions and Second Phase Particles on Hydrogen-Induced Blistering in Iron”, *Materials Chemistry and Physics*, Vol. 107, No. 2-3, 2008, pp. 231-235, doi: 10.1016/j.matchemphys.2007.07.004
- [22] Rösler M., Garcia de Albo F. J., „Contribution of Charge-Transfer Processes to Ion-Induced Electron Emission”, *Physical Review B*, Vol. 54, No. 23, 1996, pp. 17158-17165, doi: 10.1103/PhysRevB.54.17158
- [23] Sols F., Flores F., "Charge Transfer Processes for Light Ions Moving in Metals", *Physical Review B*, Vol. 30, No. 8, pp. 4878-4880, doi: 10.1103/PhysRevB.30.4878
- [24] Sznajder M., "Degradation studies of materials under space conditions; under special emphasize of recombination processes", Ph.D. Dissertation, Institute of Physics and Astronomy, University of Zielona Góra, Poland, 2013
- [25] Thomas G. J., Drotning W. D., "Hydrogen Induced Lattice Expansion in Nickel", *Metallurgical Transactions A*, Vol. 14, No. 8, 1983, pp. 1545-1548, doi: 10.1007/BF02654380
- [26] Ziegler J. F., SRIM Software, www.srim.org